



Structure, DNA- and albumin-binding of the manganese(II) complex with the non-steroidal antiinflammatory drug niflumic acid

Paulina Tsiliki^a, Franc Perdih^b, Iztok Turel^b, George Psomas^{a,*}

^a Department of General and Inorganic Chemistry, Faculty of Chemistry, Aristotle University of Thessaloniki, GR-54124 Thessaloniki, Greece

^b Faculty of Chemistry and Chemical Technology, University of Ljubljana, Askerceva 5, 1000 Ljubljana, Slovenia

ARTICLE INFO

Article history:

Received 18 December 2012

Accepted 29 January 2013

Available online 8 February 2013

Keywords:

Manganese(II) complexes

Non-steroidal antiinflammatory drugs

Niflumic acid

Interaction with DNA

Interaction with albumins

ABSTRACT

The manganese(II) complex with the non-steroidal antiinflammatory drug niflumic acid has been synthesized and characterized. The crystal structure of the complex $[\text{Mn}(\text{O-niflumato})_2(\text{methanol})_4]$ has been determined by X-ray crystallography, where a monodentate coordination of niflumato ligand was revealed. Niflumic acid and its Mn(II) complex exhibit good binding affinity to human or bovine serum albumin proteins with high binding constant values. UV study of the interaction of the compounds with calf-thymus DNA (CT DNA) has shown that the compounds can bind to CT DNA and $[\text{Mn}(\text{O-niflumato})_2(-\text{methanol})_4]$ exhibits higher binding constant to CT DNA than free niflumic acid. The compounds can bind to CT DNA via intercalation as concluded by DNA solution viscosity measurements. Competitive studies with ethidium bromide (EB) have shown that the compounds can displace the DNA-bound EB suggesting strong competition with EB.

© 2013 Elsevier Ltd. All rights reserved.

1. Introduction

Non-steroidal antiinflammatory drugs (NSAIDs), among the most used analgesic, antiinflammatory and antipyretic agents [1], act through inhibition of the cyclo-oxygenase (COX)-mediated production of prostaglandins [2], while they have also presented a synergistic role on the activity of certain antitumor drugs leading a series of cancer cell lines to cell death via apoptosis [3]. As a means to explain the tentative anticancer and antiinflammatory activity of the NSAIDs and their complexes, the interaction with DNA is considered of great importance and should be further evaluated, although few relevant reports on the interaction of NSAIDs and their complexes with DNA have been published so far [4,5].

The chemical classes of NSAIDs comprise phenylalkanoic acids, salicylate derivatives, anthranilic acids, oxicams, sulfonamides and furanones [6]. Niflumic acid (=Hnif, Scheme 1) is a NSAID of N-phenylanthranilic acid derivatives and resembles chemically to mefenamic, tolfenamic and flufenamic acid and other fenamates in clinical use [6]. Hnif is used to treat inflammatory rheumatoid

diseases and relieve acute pain and it is effective against period pains, pain after surgery, and fever [7,8]. The crystal structures of two dinuclear [8,9] and two mononuclear copper(II) complexes [10,11] and a silver(I) [12] complex of niflumic acid have been reported in the literature.

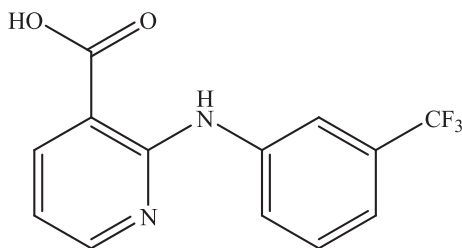
Manganese, one of the most significant biometals, is found in the active center of many enzymes of diverse functionality [13,14]. It is known that, like many other metal ions, also hydrated manganese(II) ions interact with DNA [15]. The crystal structure of oligonucleotide in the presence of manganese(II) revealed among other the involvement of the metal in the formation of cross-links between neighbor duplexes [16]. The crystal structure of nucleosome core particle has shown that manganese(II) interacts with N7 atom of guanines and adenines [17]. Manganese-containing compounds SC-52608 and Teslascan are used in medicine as anticancer and MRI contrast agents, respectively [18], and an increasing number of manganese complexes exhibit biological interest showing antibacterial [19,20], anticancer [21–23] and antifungal [24] activity. Furthermore, a thorough search of the literature has not revealed any structurally characterized manganese complexes with NSAIDs.

The interaction of carboxylate-containing non-steroidal antiinflammatory drugs with Co^{2+} , Cu^{2+} and Zn^{2+} [25–32] has been the subject of our recent studies covering the characterization of the resultant complexes and the interaction of these metal complexes with biomolecules such as DNA and serum albumin proteins, in an attempt to examine their mode of binding and possible biological relevance. Having in mind the significance of NSAIDs in medicine, the activity of manganese complexes and potential synergetic

Abbreviations: bipy, 2,2'-bipyridine; CT, calf-thymus; bipyam, 2,2'-bipyridylamine; BSA, bovine serum albumin; COX, cyclo-oxygenase; DMF, N,N-dimethylformamide; DMSO, dimethylsulfoxide; EB, ethidium bromide, 3,8-diamino-5-ethyl-6-phenyl-phenanthridinium bromide; Hnif, niflumic acid, 2-[3-(trifluoromethyl)anilino]nicotinic acid; HSA, human serum albumin; NSAID, non-steroidal antiinflammatory drug; phen, 1,10-phenanthroline; py, pyridine; SA, serum albumin; sh, shoulder; vs, very strong; Δ , $\nu_{\text{asym}}(\text{CO}_2)$ – $\nu_{\text{sym}}(\text{CO}_2)$.

* Corresponding author. Tel.: +30 2310997790; fax: +30 2310997738.

E-mail address: gepsomas@chem.auth.gr (G. Psomas).



Scheme 1. Niflumic acid (=Hnif).

effects, we present the synthesis and the structural characterization of the mononuclear Mn(II) complex with the NSAID niflumic acid $[\text{Mn}(\text{nif})_2(\text{MeOH})_4]$, **1**. The crystal structure of complex **1** has been determined by X-ray crystallography. Additionally, the biological properties of complex **1** including its binding to CT DNA investigated by UV spectroscopy and viscosity measurements, its ability to displace ethidium bromide (EB) as a means to investigate the existence of a potential intercalation to CT DNA in competition to the classical DNA-intercalator EB studied by fluorescence spectroscopy, and its affinity to bovine (BSA) and human serum albumin (HSA) – binding to these proteins involved in the transport of metal ions and metal–drug complexes through the blood stream may result in lower or enhanced biological properties of the original drug, or new paths for drug transportation – investigated by fluorescence spectroscopy, have been evaluated and compared to those of free niflumic acid.

2. Experimental

2.1. Materials – instrumentation – physical measurements

Niflumic acid, $\text{MnCl}_2 \cdot 4\text{H}_2\text{O}$, 2,2'-bipyridylamine (=bipyam), 1,10-phenanthroline (=phen), 2,2'-bipyridine (=bipy), KOH, trisodium citrate, NaCl, CT DNA, BSA, HSA and EB were purchased from Sigma–Aldrich Co and all solvents were purchased from Merck. All chemicals and solvents were reagent grade and were used as purchased.

DNA stock solution was prepared by dilution of CT DNA to buffer (containing 150 mM NaCl and 15 mM trisodium citrate at pH 7.0) followed by exhaustive stirring at 4 °C for three days, and kept at 4 °C for no longer than a week. The stock solution of CT DNA gave a ratio of UV absorbance at 260 and 280 nm (A_{260}/A_{280}) of 1.88, indicating that the DNA was sufficiently free of protein contamination. The DNA concentration was determined by the UV absorbance at 260 nm after 1:20 dilution using $\epsilon = 6600 \text{ M}^{-1} \text{ cm}^{-1}$ [26–28].

Infrared (IR) spectra ($400\text{--}4000 \text{ cm}^{-1}$) were recorded on a Nicolet FT-IR 6700 spectrometer with samples prepared as KBr pellets. UV–Visible (UV–Vis) spectra were recorded as nujol mulls and in solution at concentrations in the range $10^{-5}\text{--}10^{-3} \text{ M}$ on a Hitachi U-2001 dual beam spectrophotometer. Room temperature magnetic measurements were carried out on a magnetic susceptibility balance of Sherwood Scientific (Cambridge, UK). C, H and N elemental analysis were performed on a Perkin–Elmer 240B elemental analyzer. Molar conductivity measurements were carried out in 1 mM DMSO solution of the complexes with a Crison Basic 30 conductometer. Fluorescence spectra were recorded in solution on a Hitachi F-7000 fluorescence spectrophotometer. Viscosity experiments were carried out using an ALPHA L Fungilab rotational viscometer equipped with an 18 mL LCP spindle.

2.2. Synthesis of $[\text{Mn}(\text{nif})_2(\text{MeOH})_4]$, **1**

A methanolic solution (10 mL) containing niflumic acid (0.4 mmol, 112 mg) and KOH (0.4 mmol, 22 mg) was stirred for

1 h. The solution was added dropwise to a methanolic solution (10 mL) of $\text{MnCl}_2 \cdot 4\text{H}_2\text{O}$ (0.2 mmol, 40 mg). Colorless crystals of $[\text{Mn}(\text{nif})_2(\text{MeOH})_4]$ **1** suitable for X-ray structure determination were collected after a few days. Yield: 105 mg, 70%. *Anal. Calc.* for $[\text{Mn}(\text{nif})_2(\text{MeOH})_4]$ ($\text{C}_{30}\text{H}_{32}\text{F}_6\text{MnN}_4\text{O}_8$) (MW = 745.54): C, 48.33; H, 4.33; N, 7.52. Found: C, 47.69; H, 4.12; N, 7.25%. IR (KBr pellet): $\nu_{\text{max}}/\text{cm}^{-1}$ $\nu_{\text{asym}}(\text{CO}_2)$: 1606 (very strong (vs)); $\nu_{\text{sym}}(-\text{CO}_2)$: 1389 (vs); $\Delta = \nu_{\text{asym}}(\text{CO}_2) - \nu_{\text{sym}}(\text{CO}_2)$: 217 cm^{-1} ; UV–Vis: λ/nm ($\epsilon/\text{M}^{-1} \text{ cm}^{-1}$) as nujol mull: 327, 296; in DMSO: 331 (sh) (4500), 295 (22 500). $\mu_{\text{eff}} = 5.95 \text{ BM}$ at room temperature. The complex is soluble in DMF and DMSO ($\Lambda_{\text{M}} = 7 \text{ mho cm}^2 \text{ mol}^{-1}$, in 1 mM DMSO solution).

The addition of an N,N'-donor ligand such as bipy (0.2 mmol, 31 mg), phen (0.2 mmol, 36 mg) or bipyam (0.2 mmol, 34 mg) to the reaction solution has resulted in the isolation of crystalline product of complex **1**, and no coordination of the N,N'-donor was observed.

2.3. X-ray structure determination

Single-crystal X-ray diffraction data were collected at room temperature on an Agilent Technologies SuperNova Dual with an Atlas detector using mirror-monochromatized Mo $K\alpha$ radiation ($\lambda = 0.71073 \text{ \AA}$). The data were processed using CRYSTALIS PRO [33]. Structure was solved by direct methods implemented in SIR97 [34] and refined by a full-matrix least-squares procedure based on F^2 with SHELXL-97 [35]. All non-hydrogen atoms were refined anisotropically. All hydrogen atoms were readily located in difference Fourier maps and were subsequently treated as riding atoms in geometrically idealized positions with $U_{\text{iso}}(\text{H}) = kU_{\text{eq}}(\text{C, N})$, where $k = 1.5$ for NH and methyl groups, which were permitted to rotate but not to tilt, and 1.2 for all other H atoms. Hydrogen atoms bonded to methanol O3 and O4 atoms were refined using DFIX instruction. The $-\text{CF}_3$ group is disordered over two positions in ratio 0.59:0.41. Crystallographic data are listed in Table 1.

2.4. Albumin binding studies

Protein binding studies have been performed by tryptophan fluorescence quenching experiments using bovine (BSA, 3 μM) or human serum albumin (HSA, 3 μM) in buffer (containing 15 mM trisodium citrate and 150 mM NaCl at pH 7.0). The quenching of the emission intensity of BSA or HSA tryptophan residues at 343 nm or 351 nm, respectively, was monitored using Hnif and complex **1** as quenchers with increasing concentration (up to

Table 1
Crystallographic data for complex **1**.

	Complex 1
Formula	$\text{C}_{30}\text{H}_{32}\text{F}_6\text{MnN}_4\text{O}_8$
Fw	745.54
T (K)	293(2)
Crystal system	orthorhombic
Space group	<i>Pbca</i>
a (Å)	16.1718(3)
b (Å)	9.8618(2)
c (Å)	21.0311(4)
α (°)	90.00
β (°)	90.00
γ (°)	90.00
Volume (Å ³)	3354.10(11)
Z	4
D (calc) (Mg m^{-3})	1.476
Abs. coef., μ (mm^{-1})	0.481
GOF on F^2	1.046
R_1	0.0364 ^a
wR_2	0.0907

^a 3023 reflections with $I > 2\sigma(I)$.

2.2×10^{-5} M) [36]. Fluorescence spectra were recorded from 300 to 500 nm at an excitation wavelength of 296 nm. The compounds do not emit any significant fluorescence under the same experimental conditions. The Stern–Volmer and Scatchard equations and graphs have been used in order to study the interaction of each quencher with serum albumins.

2.5. DNA-binding studies

The interaction of Hnif and complex **1** with CT DNA has been studied with UV spectroscopy in order to investigate the possible binding modes to CT DNA and to calculate the binding constants to CT DNA (K_b). In UV titration experiments, the spectra of CT DNA in the presence of each compound have been recorded for a constant CT DNA concentration in diverse [compound]/[CT DNA] mixing ratios (r). The binding constants, K_b , of the compounds with CT DNA have been determined using the UV spectra of the compound recorded for a constant concentration in the absence or presence of CT DNA for diverse r values. Control experiments with DMSO were performed and no changes in the spectra of CT DNA were observed.

Viscosity experiments were carried out using an ALPHA L Fun-gilab rotational viscometer equipped with an 18 mL LCP spindle and the measurements were performed at 100 rpm. The viscosity of a DNA solution has been measured in the presence of increasing amounts of the compounds. The relation between the relative solution viscosity (η/η_0) and DNA length (L/L_0) is given by the equation $L/L_0 = (\eta/\eta_0)^{1/3}$, where L_0 denotes the apparent molecular length in the absence of the compound [27–29]. The obtained data are presented as $(\eta/\eta_0)^{1/3}$ versus r , where η is the viscosity of DNA in the presence of the compound, and η_0 is the viscosity of DNA alone in buffer solution.

The competitive studies of each compound with EB have been investigated with fluorescence spectroscopy in order to examine whether the compound can displace EB from its CT DNA–EB complex. The CT DNA–EB complex was prepared by adding 20 μ M EB and 26 μ M CT DNA in buffer (150 mM NaCl and 15 mM trisodium citrate at pH 7.0). The intercalating effect of the compounds with the DNA–EB complex was studied by adding a certain amount of a solution of the compound step by step into the solution of the DNA–EB complex. The influence of the addition of each compound to the DNA–EB complex solution has been obtained by recording the variation of fluorescence emission spectra.

3. Results and discussion

3.1. Synthesis and spectroscopy

Complex **1** has been synthesized under aerobic conditions with the addition of $MnCl_2$ to deprotonated niflumic acid. The complex has been also isolated in the presence of an N,N' -donor ligand such as bipy, phen or bipyam; the N,N' -donor ligand was not coordinated to manganese as concluded by IR spectroscopy and X-ray crystallography. Complex **1** is soluble in DMSO and DMF and is not electrolyte ($\Lambda_M = 7$ mho cm^2 mol^{-1} , in 1 mM DMSO solution; a value indicative of non-dissociation in DMSO solution).

The deprotonation and binding mode of niflumic acid has been confirmed by IR spectroscopy. In the IR spectrum of Hnif, the absorption band at 3379(br, m) cm^{-1} , attributed to the $\nu(H-O)$ stretching vibration disappears upon binding to manganese. The bands at 1663(s) cm^{-1} and 1284(s) cm^{-1} attributed to $\nu(C=O)_{carboxylic}$ and $\nu(C-O)_{carboxylic}$ stretching vibrations of the carboxylic moiety ($-COOH$), respectively, shift in the IR spectra of the complex at 1606 cm^{-1} and 1389 cm^{-1} assigned to the antisymmetric, $\nu_{asym}(C=O)$, and the symmetric, $\nu_{sym}(C=O)$, stretching vibrations

of the carboxylate group, respectively. The difference $\Delta [=\nu_{asym}(C=O) - \nu_{sym}(C=O)]$ is a useful characteristic tool for determining the coordination mode of the carboxylate ligands and has a value of 217 cm^{-1} which is indicative of monodentate binding mode for the niflumato ligands [37].

The UV–Vis spectra of complex **1** have been recorded as nujol mull and in DMSO solution (Fig. S1) and are similar suggesting that it retains its structure in solution. In these spectra, two bands attributed to intraligand transitions appeared. In addition, the fact that the complex has the same UV–Vis spectral pattern in nujol and in DMSO solution as well as in the presence of the buffer solution used in the biological experiments in combination to the molar conductivity measurements suggests that it keeps its integrity in solution [28].

The observed value of μ_{eff} (=5.95 BM) for the complex is close to the spin-only value (=5.92 MB) at room temperature and typical for mononuclear high-spin Mn(II) complexes with d^5 configuration ($S = 5/2$) [38,39].

3.2. Description of the crystal structure of $[Mn(niflumato)_2(MeOH)_4]$

A diagram of **1** is shown in Fig. 1, and selected bond distances and angles are listed in Table 2. The complex is mononuclear with the niflumato ligand behaving as a monodentate deprotonated ligand coordinated to manganese atom via a carboxylate oxygen.

The structure of the complex is centrosymmetric, the manganese(II) ion is sitting on a center of symmetry and is coordinated to two niflumato ligands and four methanol molecules related by the inversion center. Thus, the manganese atom is six-coordinate and displays an octahedral geometry. All the Mn–O distances are typical of Mn(II)–O bond distances with the Mn– $O_{carboxylate}$ (Mn(1)–O(1) = 2.1287(11) Å) being shorter than the Mn– $O_{methanol}$ (Mn(1)–O(3) = 2.1923(12), Mn(1)–O(4) = 2.2148(13) Å). Taking into account the differences found in the Mn–O distances in combination with the angles around manganese (O(1)–Mn(1)–O(3) = 92.20(5)°, O(1)–Mn(1)–O(4) = 89.38(5)° and O(3)–Mn(1)–O(4) = 90.56(5)°), the octahedron displays a slight distortion.

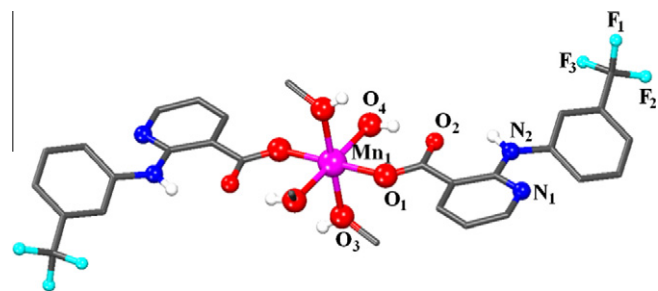


Fig. 1. The molecular structure of **1** with only the heteroatoms labelled. Hydrogens and atoms in disorder are omitted for clarity.

Table 2
Selected bond distances and angles for complex **1**.

Distance	(Å)	Distance	(Å)
Mn(1)–O(1)	2.1287(11)	Mn(1)–O(3)	2.1923(12)
Mn(1)–O(4)	2.2148(13)		
O(2)–C(1)	1.253(2)	O(1)–C(1)	1.2615(19)
O(4)–C(15)	1.420(3)	O(3)–C(14)	1.406(2)
Angle	(°)	Angle	(°)
O(1)–Mn(1)–O(1)	180.00(7)	O(3)–Mn(1)–O(3)	180.00(8)
O(1)–Mn(1)–O(3)	92.20(5)	O(3)–Mn(1)–O(4)	89.44(5)
O(1)–Mn(1)–O(3)	87.80(5)	O(3)–Mn(1)–O(4)	90.56(5)
O(1)–Mn(1)–O(4)	89.38(5)	O(4)–Mn(1)–O(4)	180.00(9)
O(1)–Mn(1)–O(4)	90.62(5)		

Table 3
Hydrogen bonding interactions in **1**.

D–H...A	D–H (Å)	H...A (Å)	D...A (Å)	D–H...A (°)	Symmetry transformation for acceptors
N(2)–H(2A)...O(2)	0.86	1.96	2.6264(18)	133.6	x, y, z
O(3)–H(1)...N(1)	0.826(10)	1.972(11)	2.7916(18)	171(3)	$x, y + 1, z$
O(4)–H(2)...O(2)	0.832(10)	0.832(10)	2.6254(16)	161(2)	x, y, z

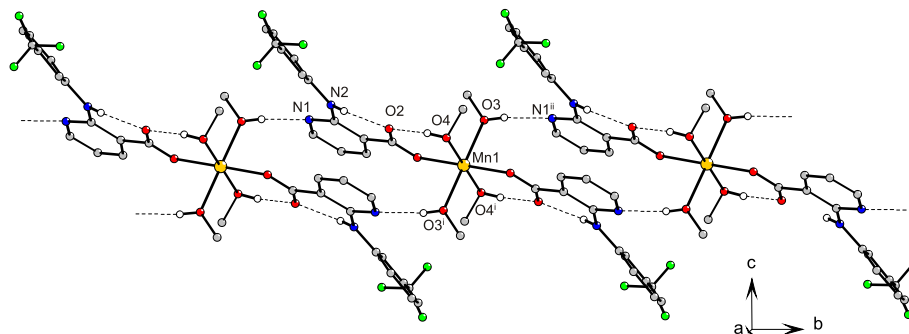


Fig. 2. Hydrogen bonding in **1**. Disorder on $-\text{CF}_3$ group and hydrogen atoms not involved in the motif shown have been omitted for clarity. Symmetry codes: (i) $-x, -y, -z$; (ii) $x, y + 1, z$.

The carboxylate group is asymmetrically bound to manganese ($\text{C}(1)–\text{O}(1) = 1.2615(9) \text{ \AA}$ and $\text{C}(1)–\text{O}(2) = 1.253(2) \text{ \AA}$). Similar arrangement of a monodentate carboxylate NSAID around the central metal ion has been also observed in the crystal structure of $[\text{Co}(\text{O}-\text{mefenamato})_2(\text{MeOH})_4]$ [26].

The structure of **1** is stabilized by intramolecular $\text{O}-\text{H} \cdots \text{O}$ and $\text{N}-\text{H} \cdots \text{O}$ hydrogen bonding between methanolic or NH group as hydrogen-bond donors and the carbonyl moiety of the niflumato ligand as hydrogen bonding acceptor (Table 3). An infinite chain is formed due to $\text{O}-\text{H} \cdots \text{N}$ intermolecular hydrogen bonding between methanolic group and the aromatic nitrogen atom of the niflumato ligand (Fig. 2).

3.3. Interaction with serum albumins

Serum albumin (SA) is the most abundant protein in plasma; its main role is the transport of metal ions, drugs and their metal complexes through the blood stream [40]. Human serum albumin (HSA) has a tryptophan at position 214 and its most extensively studied structural homolog bovine serum albumin (BSA) has two tryptophans, Trp-134 and Trp-212 [41]. HSA and BSA solutions exhibit, when excited at 295 nm, an intense fluorescence emission with $\lambda_{\text{em,max}} = 351 \text{ nm}$ and 343 nm , respectively, which is attributed to the tryptophans [36]. Hnif and complex **1** do not emit any significant fluorescence under the same experimental conditions and the quenching occurring in the HSA or BSA fluorescence emission spectra upon addition of Hnif or **1** (Fig. 3) are primarily due to change in protein conformation, subunit association, substrate binding or denaturation [41].

Addition of Hnif and complex **1** to SA solution results in moderate to significant quenching of HSA fluorescence at $\lambda = 351 \text{ nm}$ (Fig. 4(A)) (quenching of 62% of the initial fluorescence intensity for Hnif and 79% for **1**) and to a much more enhanced quenching of the BSA fluorescence at $\lambda = 343 \text{ nm}$ (Fig. 4(B)) (quenching of 86% of the initial fluorescence intensity for Hnif and 98% for **1**). The observed quenching may be due to possible changes in protein secondary structure leading to changes in tryptophan environment of HSA, and thus indicating the binding of each complex to the albumins [42].

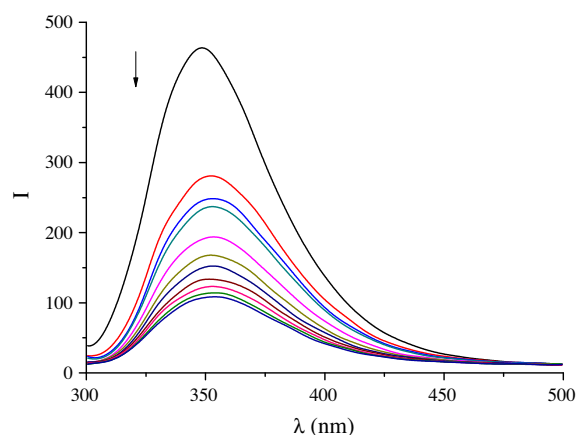


Fig. 3. Emission spectra ($\lambda_{\text{excit}} = 295 \text{ nm}$) of HSA ($[\text{HSA}] = 3 \mu\text{M}$) in buffer solution in the absence and presence of increasing amounts of complex **1** ($r = [\mathbf{1}]/[\text{HSA}] = 0-6$). The arrow shows the changes of intensity upon increasing amounts of **1**.

The Stern–Volmer and Scatchard equations and graphs are used in order to evaluate the interaction of a quencher with serum albumins. From Stern–Volmer quenching equation [36]:

$$\frac{I_0}{I} = 1 + k_q t_0 [\text{Q}] = 1 + K_{\text{SV}} [\text{Q}] \quad (1)$$

where I_0 = the initial tryptophan fluorescence intensity of SA, I = the tryptophan fluorescence intensity of SA after the addition of the quencher (i.e. Hnif and complex **1**), k_q = the quenching rate constants of SA, K_{SV} = the dynamic quenching constant, τ_0 = the average lifetime of SA without the quencher and $[\text{Q}]$ = the concentration of the quencher, the dynamic quenching constant (K_{SV} , in M^{-1}) can be obtained by the slope of the diagram $\frac{I_0}{I}$ versus $[\text{Q}]$ (Figs. S2 and S3). From the equation $K_{\text{SV}} = k_q \tau_0$ and taking as fluorescence lifetime (τ_0) of tryptophan in SA at $\sim 10^{-8} \text{ s}$ [43], the approximate quenching constant (k_q , in $\text{M}^{-1} \text{ s}^{-1}$) may also be calculated. The calculated values of K_{SV} and k_q for the interaction of the compounds with HSA and BSA are given in Table 4 suggesting good binding propensity of the compounds with complex **1** exhibiting higher SA quenching ability than free Hnif. The k_q values ($>10^{12} \text{ M}^{-1} \text{ s}^{-1}$) of the compounds are higher than diverse kinds of quenchers for biopolymers

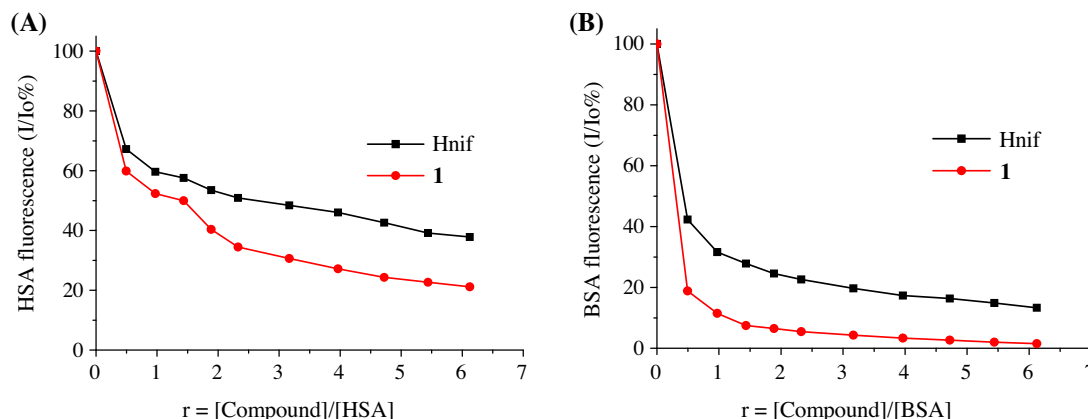


Fig. 4. Plot of % relative fluorescence intensity at (A) $\lambda_{em} = 351$ nm (%) versus r ($r = [\text{complex}]/[\text{HSA}]$) and (B) $\lambda_{em} = 343$ nm (%) versus r ($r = [\text{complex}]/[\text{BSA}]$), for Hnif and complex **1** in buffer solution (150 mM NaCl and 15 mM trisodium citrate at pH 7.0).

Table 4

The SA constants and parameters derived for Hnif and complex **1**.

Compound		K_{sv} (M^{-1})	k_q ($M^{-1} s^{-1}$)	K (M^{-1})	n
HSA	Hnif	$7.48(\pm 0.35) \times 10^4$	$7.48(\pm 0.35) \times 10^{12}$	$4.14(\pm 0.36) \times 10^5$	0.66
	$[\text{Mn}(\text{nif})_2(\text{H}_2\text{O})_4]$, 1	$1.96(\pm 0.08) \times 10^5$	$1.96(\pm 0.08) \times 10^{13}$	$3.80(\pm 0.16) \times 10^5$	0.89
BSA	Hnif	$3.09(\pm 0.21) \times 10^5$	$3.09(\pm 0.21) \times 10^{13}$	$1.18(\pm 0.07) \times 10^6$	0.88
	$[\text{Mn}(\text{nif})_2(\text{H}_2\text{O})_4]$, 1	$3.11(\pm 0.07) \times 10^6$	$3.11(\pm 0.07) \times 10^{14}$	$2.89(\pm 0.09) \times 10^6$	1.00

fluorescence ($\sim 2.0 \times 10^{10} M^{-1} s^{-1}$) indicating the existence of a static quenching mechanism [41].

From the Scatchard equation [36]:

$$\frac{\Delta I/I_0}{[Q]} = nK - K \frac{\Delta I}{I_0} \quad (2)$$

where n is the number of binding sites per albumin and K is the association binding constant, K (in M^{-1}) may be calculated from the slope in plots $\frac{\Delta I/I_0}{[Q]}$ versus $\frac{\Delta I}{I_0}$ (Figs. S4 and S5) and n is given by the ratio of y intercept to the slope [36]. The results concerning the K and n values are given in Table 4, showing that for HSA Hnif exhibits higher K value and for BSA **1** does. Additionally, the n value of Hnif increases for the SA when coordinated to Mn(II).

In conclusion, the compounds exhibit higher K values for BSA than for HSA. In general, the binding constant of a compound to a protein such as an albumin should be at an optimum range; it should be (a) high enough to allow binding and possible transfer by the protein and (b) not too high so that it can be released upon arrival at its target(s). Bearing that in mind, the K values of the compounds may be considered to be within such a range; high enough (3.80×10^5 – $2.89 \times 10^6 M^{-1}$) to allow the binding of the complexes to SAs and also significantly below the association constant of one of strongest known non-covalent bonds for the interaction between avidin and ligands ($K \approx 10^{15} M^{-1}$), suggesting a possible release from the serum albumin to the target cells [42].

3.4. Interaction with calf-thymus DNA

The potential anticancer and the antiinflammatory activity of the NSAIDs and their complexes may be often related to their ability to interact with DNA [4,5]. Nevertheless, the number of such studies so far is limited; the interaction of DNA with a series of copper(II) and cobalt(II) complexes with the NSAIDs naproxen, diclofenac, mefenamic acid and diflunisal has been recently reported by our lab [25–30], while complexes of oxycams are reported to bind to DNA via intercalation [5]. As known, transition metal ions

and complexes can bind to DNA via a covalent (a labile ligand of the complex is replaced by a nitrogen base of DNA, e.g. guanine N7) and/or a noncovalent (intercalation, electrostatic or groove binding) interaction [25–30].

The UV spectra of a CT DNA solution with standard concentration ($2 \times 10^{-4} M$) have been recorded upon addition Hnif or complex **1** at different [compound]/[DNA] mixing ratios (r). The changes observed are similar and UV spectra of a CT DNA solution upon addition of Hnif are shown representatively in Fig. 5(A). The decrease of the intensity at $\lambda_{max} = 257$ nm is accompanied with a red-shift of the λ_{max} up to 263 nm for both compounds, indicating that the interaction with CT DNA results in the direct formation of a new complex with double-helical CT DNA [44]. The observed hypochromism may be attributed to $\pi \rightarrow \pi^*$ stacking interaction between the aromatic chromophore from niflumato ligands and DNA base pairs consistent with the intercalative binding mode [45] and the accompanying bathochromism may be considered an evidence of stabilization of CT DNA duplex [46].

In the UV region of the spectra ($10^{-5} M$) of the compounds, the observed absorption bands are mainly attributed to intraligand transitions of the NSAID ligands [25–30]. The existence and the possible mode of interaction between each compound and CT DNA may be revealed by the changes in the intraligand centered spectral transitions upon addition of CT DNA solution in diverse r values. More specifically, in the UV spectrum of Hnif (Fig. 5(B)), the band centered at 340 nm exhibits in the presence of increasing amounts of CT DNA a significant hypochromism up 30% suggesting tight binding to CT DNA probably by intercalation. Further addition of DNA results in a gradual elimination of this band. A distinct isosbestic point at 335 nm appears upon addition of CT DNA. In the UV spectrum of **1** (Fig. 5(C)), the bands centered at 331 nm (band I) and 295 nm (band II) exhibit in the presence of increasing amounts of CT DNA a slight hypochromism as an evidence of tight binding.

Although the exact mode of binding cannot be merely proposed by UV spectroscopic titration studies, the results collected from the UV titration experiments suggest that both compounds can bind to

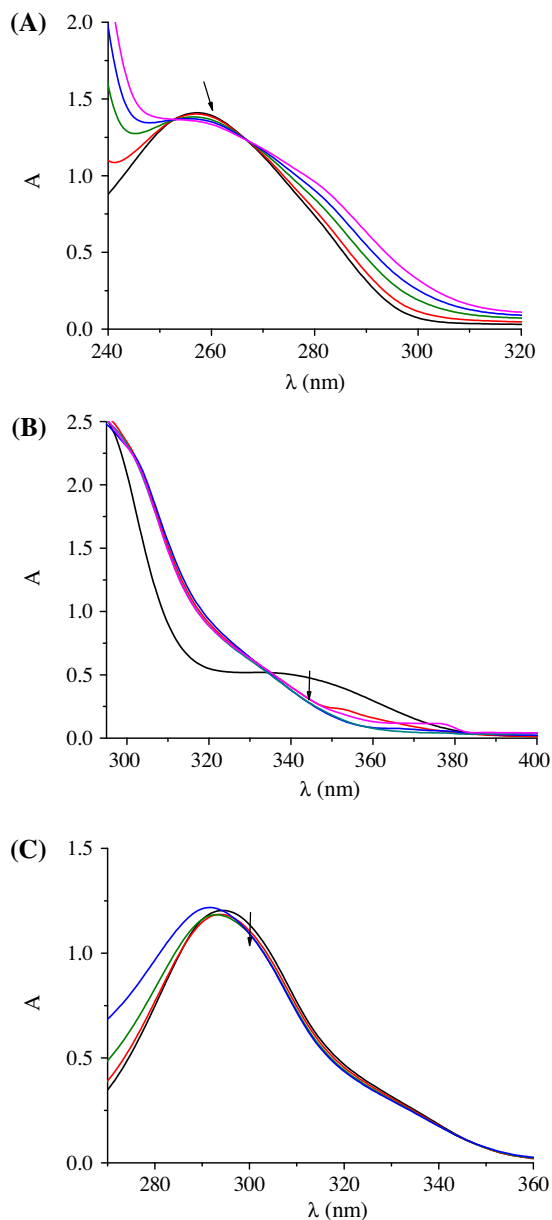


Fig. 5. (A) UV spectra of CT DNA (2×10^{-4} M) in buffer solution (150 mM NaCl and 15 mM trisodium citrate at pH 7.0) in the absence or presence of Hnif. The arrow shows the changes upon increasing amounts of Hnif. (B) and (C) UV spectra of a DMSO solution (10^{-5} M) of (B) Hnif and (C) $[\text{Mn}(\text{nifl})_2(\text{H}_2\text{O})_4]$, **1** in the presence of CT DNA at increasing amounts. The arrows show the changes upon increasing amounts of CT DNA.

CT DNA [47]. The observed hypochromic effect may be considered as first evidence of tight binding to CT DNA probably by intercalation and a stabilization of the DNA double helix [48].

The magnitude of the binding strength of compounds to CT DNA can be evaluated through the calculation of the binding constant K_b , which is obtained by monitoring the changes in the absorbance at the corresponding λ_{max} with increasing concentrations of CT DNA. K_b (in M^{-1}) is given by the ratio of slope to the y intercept in plots $\frac{[\text{DNA}]}{(\varepsilon_A - \varepsilon_f)}$ versus [DNA] (Fig. S6), according to the equation [45]:

$$\frac{[\text{DNA}]}{(\varepsilon_A - \varepsilon_f)} = \frac{[\text{DNA}]}{(\varepsilon_b - \varepsilon_f)} + \frac{1}{K_b(\varepsilon_b - \varepsilon_f)} \quad (3)$$

where [DNA] is the concentration of DNA in base pairs, $\varepsilon_A = A_{\text{obsd}}/[\text{compound}]$, ε_f = the extinction coefficient for the free compound

Table 5

The DNA binding constants (K_b) and Stern–Volmer constants (K_{SV}) of EB–DNA fluorescence for Hnif and complex **1**.

Compound	K_b (M^{-1})	K_{SV} (M^{-1})
Hnif	$7.60(\pm 0.13) \times 10^5$	$1.54(\pm 0.03) \times 10^6$
$[\text{Mn}(\text{nifl})_2(\text{H}_2\text{O})_4]$, 1	$8.67(\pm 0.22) \times 10^5$	$1.82(\pm 0.03) \times 10^6$

and ε_b = the extinction coefficient for the compound in the fully bound form. The values of K_b for the compound, as calculated by Eq. (3) and the plots in Fig. S6, are given in Table 5. The K_b values are considered high suggesting a strong binding of the compounds to CT DNA [26–29]. Upon coordination of niflumic acid to Mn(II), an increase of the K_b value may be observed. The K_b values of both compounds are higher than that of the classical intercalator EB ($K_b = 1.23(\pm 0.07) \times 10^5 \text{ M}^{-1}$) [26–29].

The measurement of the viscosity of DNA solution upon addition of a compound may provide significant aid to clarify the interaction mode of a compound with DNA, since DNA viscosity is sensitive to DNA length changes [26–29]. In the case of classic intercalative binding mode, the insertion of the compound in between the DNA base pairs results in an increase in the separation of base pairs at intercalation sites in order to host the bound compound; therefore, the increase of the length of the DNA helix will be obvious through an increase of DNA viscosity, the magnitude of which is usually in accordance to the strength of the interaction. Furthermore, the binding of a compound to DNA grooves via a partial or non-classic intercalation (i.e. electrostatic interaction or external groove-binding) may provoke a bend or kink in the DNA helix and subsequently a shortening of its effective length; as a result, the viscosity of the DNA solution may show a slight decrease or may remain unchanged [49,50].

Viscosity measurements were carried out on CT DNA solutions (0.1 mM) upon addition of increasing amounts of the compounds. The addition of the compounds results in an increase of the relative viscosity of DNA (Fig. 6) which may be an evidence of the existence of an intercalative binding mode between DNA and each compound [25–29]; a conclusion in accordance to that derived from UV spectroscopic studies.

Ethidium bromide (EB = 3,8-diamino-5-ethyl-6-phenyl-phenanthridinium bromide) is a typical indicator of intercalation [51]; it can intercalate to CT DNA via its planar EB phenanthridine ring between adjacent base pairs on the double helix, and, as a result of such an intercalation, intense fluorescence is emitted in the presence of CT DNA. Therefore, the changes observed in the fluorescence emission spectra of a solution containing EB bound to CT DNA may be used to study the interaction between DNA and

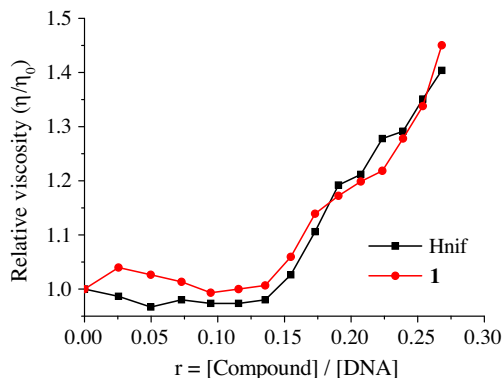


Fig. 6. Relative viscosity of CT DNA (η/η_0) in buffer solution (150 mM NaCl and 15 mM trisodium citrate at pH 7.0) in the presence of Hnif and complex **1** at increasing amounts (r).

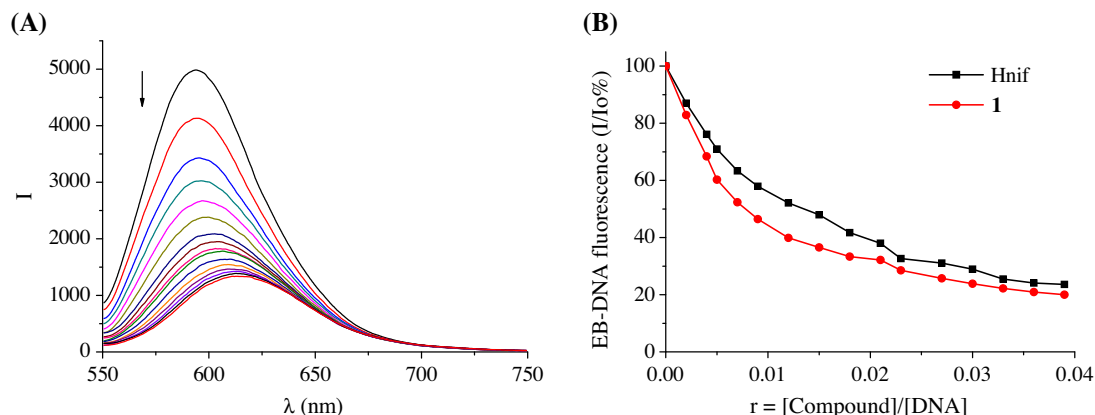


Fig. 7. (A) Emission spectra ($\lambda_{\text{excit}} = 540 \text{ nm}$) for EB–DNA ([EB] = 20 μM , [DNA] = 26 μM) in buffer solution in the absence and presence of increasing amounts of complex **1**. The arrow shows the changes of intensity upon increasing amounts of **1**. (B) Plot of EB–DNA relative fluorescence intensity (I/I_0) at $\lambda_{\text{em}} = 592 \text{ nm}$ versus r ($r = [\text{compound}]/[\text{DNA}]$) in buffer solution (150 mM NaCl and 15 mM trisodium citrate at pH 7.0) in the presence of Hnif or complex **1**.

other compounds, since the addition of a compound which could intercalate to DNA equally or more strongly than EB, should result in a quenching of the DNA-induced EB fluorescence emission (Fig. 7(A)) [52].

The emission spectra of EB bound to CT DNA in the absence and presence of each compound have been recorded for [EB] = 20 μM , [DNA] = 26 μM for increasing amounts of the compound. The addition of Hnif or complex **1** at diverse r values results in a significant decrease of the intensity of the emission band of the DNA–EB system at 592 nm (the final fluorescence is up to 24% of the initial EB–DNA fluorescence intensity for Hnif and 20% for complex **1**, (Fig. 7(B))) indicating the competition of the compounds with EB in binding to DNA. The observed significant quenching of DNA–EB fluorescence by the compounds suggests that they can displace EB from the DNA–EB complex, thus probably interacting with CT DNA by the intercalative mode [26–30].

The Stern–Volmer constant, K_{SV} (in M^{-1}), is used to evaluate the quenching ability of each compound according to the equation (Eq. (4)):

$$\frac{I_0}{I} = 1 + K_{\text{SV}}[Q] \quad (4)$$

where I_0 and I are the emission intensities in the absence and the presence of the quencher, respectively, $[Q]$ is the concentration of the quencher (Hnif or complex **1**). K_{SV} (in M^{-1}) is obtained by the slope of the diagram $\frac{I_0}{I}$ versus $[Q]$ in Stern–Volmer plots of DNA–EB. The experimental data (Fig. S7) indicate that the quenching of EB bound to DNA provoked by the compound is in good agreement ($R = 0.99$) with the linear Stern–Volmer equation (Eq. (4)). The relatively high K_{SV} (Table 5) values of the compounds show that they can bind tightly to the DNA [25–30] with complex **1** exhibiting higher K_{SV} value than free niflumic acid.

4. Conclusions

The interaction of manganese(II) with the non-steroidal anti-inflammatory drug niflumic acid results in the formation of the mononuclear complex $[\text{Mn}(\text{O-niflumato})_2(\text{O-methanol})_4]$, **1** where the niflumato ligands are bound via a carboxylato oxygen atom. The crystal structure of complex **1** has been determined by X-ray crystallography and is so far the first reported crystal structure of a Mn(II)–NSAID complex.

Niflumic acid and its Mn(II) complex show good quenching ability of the BSA and HSA fluorescence and tight binding affinity to these proteins giving relatively high binding constants. Complex

1 has higher quenching ability for the albumins' fluorescence than free Hnif.

UV spectroscopy studies and viscosity measurements have revealed the ability of the compounds to bind to CT DNA. The binding strength of the complexes with CT DNA calculated with UV spectroscopic titrations have shown that the complex $[\text{Mn}(\text{nif})_2(-\text{MeOH})_4]$ exhibits higher K_b value than that of free niflumic acid; both compounds have higher K_b values than that of EB. Competitive binding studies with EB have revealed the ability of the compounds to displace the typical intercalator EB from the EB–CT DNA complex indicating intercalation as a possible mode of their interaction with CT DNA. The intercalative binding mode has been also confirmed by viscosity measurements of CT DNA solutions in the presence of the compounds.

Acknowledgements

Financial support from the Slovenian Research Agency (ARRS) through project P1-0175 is gratefully acknowledged. The project was also supported by COST Action CM1105 and partially by the infrastructure of the EN-FIST, Center of Excellence, Ljubljana, Slovenia.

Appendix A. Supplementary data

CCDC 916035 contains the supplementary crystallographic data for this paper. These data can be obtained free of charge via <http://www.ccdc.cam.ac.uk/conts/retrieving.html>, or from the Cambridge Crystallographic Data Centre, 12 Union Road, Cambridge CB2 1EZ, UK; fax: +44 1223 336 033; or e-mail: deposit@ccdc.cam.ac.uk. Supplementary data associated with this article can be found, in the online version, at <http://dx.doi.org/10.1016/j.poly.2013.01.049>.

References

- [1] C.P. Duffy, C.J. Elliott, R.A. O'Connor, M.M. Heenan, S. Coyle, I.M. Cleary, K. Kavanagh, S. Verhaegen, C.M. O'Loughlin, R. NicAmhlaioibh, M. Clynes, *Eur. J. Cancer* 34 (1998) 1250.
- [2] A.R. Amin, P. Vyas, M. Attur, J. Leszczynskapiziak, I.R. Patel, G. Weissmann, S.B. Abramson, *Proc. Natl. Acad. Sci.* 92 (1995) 7926.
- [3] K. Kim, J. Yoon, J.K. Kim, S.J. Baek, T.E. Eling, W.J. Lee, J. Ryu, J.G. Lee, J. Lee, J. Yoo, *Biochem. Biophys. Res. Commun.* 325 (2004) 1298.
- [4] T. Zhang, T. Otevrel, Z.Q. Gao, Z.P. Gao, S.M. Ehrlich, J.Z. Fields, B.M. Boman, *Cancer Res.* 61 (2001) 8664.
- [5] S. Roy, R. Banerjee, M. Sarkar, *J. Inorg. Biochem.* 100 (2006) 1320.
- [6] J.E. Weder, C.T. Dillon, T.W. Hambly, B.J. Kennedy, P.A. Lay, J.R. Biffin, H.L. Regtop, N.M. Davies, *Coord. Chem. Rev.* 232 (2002) 95, and references therein.
- [7] J.R.J. Sorenson, *J. Med. Chem.* 19 (1976) 135.

- [8] F.T. Greenaway, E. Riviere, J.J. Girerd, X. Labouze, G. Morgant, B. Viosat, J.C. Daran, M. Roch Arveiller, N.-H. Dung, J. Inorg. Biochem. 76 (1999) 19.
- [9] B. Viosat, F.T. Greenaway, G. Morgant, J.-C. Daran, N.-H. Dung, J.R.J. Sorenson, J. Inorg. Biochem. 99 (2005) 355.
- [10] F. Valach, M. Tokarcik, P. Kubinec, M. Melnik, L. Macaskova, Polyhedron 16 (1997) 1461.
- [11] M. Koman, M. Melnik, T. Glowiak, J. Coord. Chem. 44 (1998) 133.
- [12] Y.H. Tan, S.P. Yang, Q.S. Li, Y.L. Tan, Chin. J. Struct. Chem. 25 (2006) 1387.
- [13] E.J. Larson, V.L. Pecoraro, in: V.L. Pecoraro (Ed.), Manganese Enzymes, VCH Publishers Inc., New York, 1992.
- [14] D.P. Kessissoglou, Coord. Chem. Rev. 186 (1999) 837.
- [15] I. Turel, J. Kljun, Curr. Top. Med. Chem. 11 (2011) 2661.
- [16] H. Millonig, J. Pous, C. Gouyette, J.A. Subirana, J.L. Campos, J. Inorg. Biochem. 103 (2009) 876.
- [17] J.M. Harp, B.L. Hanson, D.E. Timm, G.J. Bunick, Acta Crystallogr., Sect. D 56 (2000) 1513.
- [18] Z. Guo, P.J. Sadler, Angew. Chem., Int. Ed. 38 (1999) 1512.
- [19] P. Dorkov, I. Pantcheva, W. Sheldrick, H. Figge, R. Petrova, M. Mitewa, J. Inorg. Biochem. 102 (2008) 26.
- [20] S. Mandal, A. Rout, A. Ghosh, G. Pilet, D. Bandyopadhyay, Polyhedron 28 (2009) 3858.
- [21] M. Li, C. Chen, D. Zhang, J. Niu, B. Ji, Eur. J. Med. Chem. 45 (2010) 3169.
- [22] D. Zhou, Q. Chen, Y. Qi, H. Fu, Z. Li, K. Zhao, J. Gao, Inorg. Chem. 50 (2011) 6929.
- [23] X. Chen, L. Tang, Y. Sun, P. Qiu, G. Liang, J. Inorg. Biochem. 104 (2010) 1141.
- [24] D.P. Singh, K. Kumar, C. Sharma, Eur. J. Med. Chem. 45 (2010) 1230.
- [25] S. Tsiliou, L.-A. Kefala, F. Perdih, I. Turel, D.P. Kessissoglou, G. Psomas, Eur. J. Med. Chem. 48 (2012) 132.
- [26] F. Dimiza, A.N. Papadopoulos, V. Tangoulis, V. Psycharis, C.P. Raptopoulou, D.P. Kessissoglou, G. Psomas, Dalton Trans. 39 (2010) 4517.
- [27] F. Dimiza, A.N. Papadopoulos, V. Tangoulis, V. Psycharis, C.P. Raptopoulou, D.P. Kessissoglou, G. Psomas, J. Inorg. Biochem. 107 (2012) 54.
- [28] F. Dimiza, S. Fountoulaki, A.N. Papadopoulos, C.A. Kontogiorgis, V. Tangoulis, C.P. Raptopoulou, V. Psycharis, A. Terzis, D.P. Kessissoglou, G. Psomas, Dalton Trans. 40 (2011) 8555.
- [29] F. Dimiza, F. Perdih, V. Tangoulis, I. Turel, D.P. Kessissoglou, G. Psomas, J. Inorg. Biochem. 105 (2011) 476.
- [30] S. Fountoulaki, F. Perdih, I. Turel, D.P. Kessissoglou, G. Psomas, J. Inorg. Biochem. 105 (2011) 1645.
- [31] A. Tarushi, F. Kastanias, V. Psycharis, C.P. Raptopoulou, G. Psomas, D.P. Kessissoglou, Inorg. Chem. 51 (2012) 7460.
- [32] A. Tarushi, X. Totta, C. Raptopoulou, V. Psycharis, G. Psomas, D.P. Kessissoglou, Dalton Trans. 41 (2012) 7082.
- [33] Agilent, CRYSTALIS PRO, Agilent Technologies, Yarnton, England, 2011.
- [34] A. Altomare, M.C. Burla, M. Camalli, G.L. Casciaro, C. Giacovazzo, A. Guagliardi, A.G.G. Moliterni, G. Polidori, R. Spagna, J. Appl. Crystallogr. 32 (1999) 115.
- [35] G.M. Sheldrick, SHELXL-97, Program for the Refinement of Crystal Structures, University of Göttingen, Germany, 1997.
- [36] J.R. Lakowicz, Principles of Fluorescence Spectroscopy, third ed., Plenum Press, New York, 2006.
- [37] K. Nakamoto, Infrared and Raman Spectra of Inorganic and Coordination Compounds, Part B: Applications in Coordination, Organometallic, and Bioinorganic Chemistry, sixth ed., Wiley, New Jersey, 2009.
- [38] B. Chiswell, E.D. McKenzie, L.F. Lindoy, in: G. Wilkinson (Ed.), Comprehensive Coordination Chemistry, vol. 4, Pergamon Press, Oxford, 1987, p. 1.
- [39] D.C. Weatherburn, S. Mandal, S. Mukhopadhyay, S. Bhaduri, L.F. Lindoy, in: J.A. McCleverty, T.J. Meyer (Eds.), Comprehensive Coordination Chemistry II, vol. 5, Elsevier, 2003, p. 1.
- [40] C. Tan, J. Liu, H. Li, W. Zheng, S. Shi, L. Chen, L. Ji, J. Inorg. Biochem. 102 (2008) 347.
- [41] Y. Wang, H. Zhang, G. Zhang, W. Tao, S. Tang, J. Luminescence 126 (2007) 211.
- [42] V. Rajendiran, R. Karthik, M. Palaniandavar, H. Stoeckli-Evans, V.S. Periasamy, M.A. Akbarsha, B.S. Srinag, H. Krishnamurthy, Inorg. Chem. 46 (2007) 8208.
- [43] J.R. Lakowicz, G. Weber, Biochemistry 12 (1973) 4161.
- [44] Q. Zhang, J. Liu, H. Chao, G. Xue, L. Ji, J. Inorg. Biochem. 83 (2001) 49.
- [45] A.M. Pyle, J.P. Rehmann, R. Meshoyrer, C.V. Kumar, N.J. Turro, J.K. Barton, J. Am. Chem. Soc. 111 (1989) 3053.
- [46] E.C. Long, J.K. Barton, Acc. Chem. Res. 23 (1990) 271.
- [47] A. Jancso, L. Nagy, E. Moldrheim, E. Sletten, J. Chem. Soc., Dalton Trans. (1999) 1587.
- [48] G. Pratviel, J. Bernadou, B. Meunier, Adv. Inorg. Chem. 45 (1998) 251.
- [49] J.L. Garcia-Gimenez, M. Gonzalez-Alvarez, M. Liu-Gonzalez, B. Macias, J. Borras, G. Alzuet, J. Inorg. Biochem. 103 (2009) 923.
- [50] J. Liu, H. Zhang, C. Chen, H. Deng, T. Lu, L. Li, Dalton Trans. (2003) 114.
- [51] W.D. Wilson, L. Ratmeyer, M. Zhao, L. Strekowski, D. Boykin, Biochemistry 32 (1993) 4098.
- [52] S. Dhar, M. Nethaji, A.R. Chakravarty, J. Inorg. Biochem. 99 (2005) 805.